COMB, D. G. & ROSEMAN, S. (1958). *J. Amer. Chem. Soc.* **80**, 497–499.
COMB, D. G., WATSON, D. R. & ROSEMAN, S. (1966). *J. Biol. Chem.* **241**, 5637–5642.
DONOHUE, J. (1968). In *Structural Chemistry and Molecular Biology*, edited by A. RICH and N. DAVIDSON, pp. 443–465. San Francisco: Freeman.
GILARDI, R. D. (1973). *Acta Cryst.* To be published.
International Tables for X-ray Crystallography (1962). Vol. III, Birmingham: Kynoch Press.
IUPAC COMMISSION ON THE NOMENCLATURE OF ORGANIC CHEMISTRY AND IUPAC-IUB COMMISSION ON BIOCHEMICAL NOMENCLATURE (1972). *J. Biol. Chem.* **247**, 613–635.
JEFFREY, G. A. & ROSENSTEIN, R. D. (1964). *Advanc. Carbohydr. Chem.* **19**, 7–22.
JOHNSON, C. K. (1965). *ORTEP*. Report ORNL-3794, Oak Ridge National Laboratory, Oak Ridge, Tennessee.
JOHNSON, L. N. (1966). *Acta Cryst.* **21**, 885–891.
KARLE, J. (1968). *Acta Cryst.* B**24**, 182–186.
KARLE, J. & HAUPTMAN, H. (1950). *Acta Cryst.* **3**, 181–187.
KARLE, J. & KARLE, I. L. (1966). *Acta Cryst.* **21**, 849–859.
KEEFE, W. E. & STEWART, J. M. (1972). *Acta Cryst.* B**28**, 2469–2474.
KLYNE, W. & PRELOG, V. (1960). *Experientia*, **16**, 521.
KUHN, R. & BROSSMER, R. (1957). *Angew. Chem.* **69**, 534.
LIU, T. Y., GOTSCHLICH, E. C., DUNNE, F. T. & JONSSEN, E. K. (1971). *J. Biol. Chem.* **246**, 4703–4712.
TAKAI, M., WATANABE, S., ASHIDA, T. & KAKUDO, M. (1972). *Acta Cryst.* B**28**, 2370–2376.
YU, R. K. & LEDEEN, R. (1969). *J. Biol. Chem.* **244**, 1306–1313.

Acta Cryst. (1973). B**29**, 1886

The Crystal and Molecular Structure of Haloperidol, a Potent Psychotropic Drug

BY LARRY L. REED AND JOHN P. SCHAEFER

Department of Chemistry, University of Arizona, Tucson, Arizona 85721, *U.S.A.*

(*Received* 13 *September* 1972; *accepted* 26 *April* 1973)

The crystal and molecular structure of haloperidol has been determined using single-crystal X-ray diffraction techniques. The molecule crystallizes in the space group $P2_1/c$ in a cell of dimensions $a=7{\cdot}816$ (5), $b=8{\cdot}995$ (6), $c=28{\cdot}344$ (20) Å, $\beta=106{\cdot}34$ (4)° with $Z=4$. The structure was solved by direct methods and refined by full-matrix least-squares calculations to a final residual of 0·077.

Haloperidol[4-(4-hydroxy-4-*p*-chlorophenylpiperidino) 4′-fluorobutyrophenone, I*a*] is an extremely potent member of the butyrophenone based psychotropic drugs. The recent structure determinations of two very similar compounds, I*b* and I*b*.HCl (Koch & Germain, 1972), prompt us to report our findings for haloperidol. This structure was determined in connection with our general interest in psychotropic drugs including molecules of the thioxanthene structural type (Schaefer, 1967).

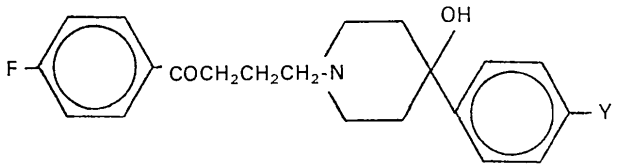

(I*a*), Y = Cl
(I*b*), Y = F

Experimental

A sample of haloperidol (HALDOL®, McNeil Laboratories) was recrystallized from ethanol–ethyl acetate.

Preliminary photographic studies showed the crystals to be monoclinic (2/*m*). The space group $P2_1/c$ was determined from the observed extinctions. Unit cell parameters, $a=7{\cdot}816$ (5), $b=8{\cdot}995$ (6), $c=28{\cdot}344$ (20) Å, $\beta=106{\cdot}34$ (4)° were obtained by least-squares, refinement of the angular parameters of several reflections accurately aligned on a Picker FACS-I four-circle diffractometer.

The calculated crystal density 1·24 g cm^{-3} based on four molecules per unit cell is in good agreement with the observed density of 1·23 g cm^{-3} determined by flotation.

Intensity data were collected on a Picker FACS-I diffractometer using monochromatic Cu $K\alpha$ radiation ($\lambda=1{\cdot}5418$ Å, graphite single-crystal monochromator) and a crystal of approximate dimensions $0{\cdot}5\times0{\cdot}2\times0{\cdot}1$ mm. The θ–2θ scanning technique involved a scan rate of 2·0° min^{-1}, covering a minimum interval width of 2·0° in 2θ (automatically adjusted to correct for dispersion). Stationary-crystal stationary-counter background measurements of 10 s duration were made at each end of the scan interval. To minimize counter coincidence losses, aluminum foil attenuators were automatically inserted in the diffracted beam whenever the counting rate exceeded $\sim10^4$ counts s^{-1}. Monitoring of equipment stability and crystal movement or decomposition was provided by the periodic collection of two standard reflections. Subsequent analysis of these standards revealed only minor fluctua-

tions ($< \pm 3\%$) in intensity as a function of time. 2851 unique data ($2\theta \leq 125°$) were collected. These data were reduced to values of F_o^2 and $\sigma(F_o^2)$ without correcting for absorption.

Solution and refinement

This structure was solved by using *MULTAN* (Germain, Main & Woolfson, 1970) and the tangent formula (Karle & Hauptman, 1956), where the phase angles $\varphi(hkl)$ are restricted to 0 or π as required by this centrosymmetric structure. Table 1 defines the initial information used to generate 288 phased normalized structure factors (E's).

Table 1. *Starting phase information for tangent formula*

	h	k	l	E	$\varphi(hkl)$
	1	1	−5	5·26	0
Origin	5	4	1	3·75	0
	3	4	10	3·54	0
Σ_1	0	2	0	4·31	0
	2	0	10	3·19	$p(0)$
Variable phases*	1	5	0	2·84	$q(0)$
	3	5	16	2·81	$r(0)$

* The variable phases p, q and r were assigned values of 0 or π in all 8 possible combinations. Values in parentheses are the phase values associated with the combination having the largest figure of merit and which yielded an E map showing the entire structure.

A subsequent E map revealed all 26 non-hydrogen atoms. Full-matrix least-squares refinement based on $|F_o|$ first with individual atom isotropic thermal parameters followed by anisotropic thermal parameters resulted in $R_1 = 0{\cdot}091$ and $R_2 = 0{\cdot}082$, where

$$R_1 = \sum||F_o| - |F_c||/\sum|F_o|$$

and

$$R_2 = [\sum w(F_o - F_c)^2/\sum wF_o^2]^{1/2}.$$

The quantity minimized is defined as $\sum w(|F_o| - |F_c|)^2$ where $\sqrt{w} \propto 1/\sigma(F_o)$, and the summation extends over 1747 data having $F_o^2 \geq 2\sigma(F_o^2)$. Values of $\sigma(F_o^2)$ were obtained from counting statistics. After inclusion of 23 hydrogen atoms (calculated coordinates), two additional refinement cycles resulted in convergence with $R_1 = 0{\cdot}077$ and $R_2 = 0{\cdot}078$. The hydrogen atoms were assigned isotropic thermal parameters of 4 Å^2 and were included as a fixed contribution to F_c in all subsequent refinement cycles. A final difference electron density synthesis did not reveal the missing hydroxyl hydrogen atom. The range of residual electron density was approximately $\pm 0{\cdot}3$ e Å^{-3}.

A final structure-factor calculation over 2851 data [which includes 1104 data with $F_o^2 < 2\sigma(F_o^2)$] resulted in $R_1 = 0{\cdot}127$ and $R_2 = 0{\cdot}081$.

The atomic scattering factors used were those tabulated by Hanson, Herman, Lea & Skillman (1964).

Discussion

Fig. 1 shows a perspective view of the molecule including the numbering scheme and final bond distances. Atomic coordinates and anisotropic thermal parameters are presented in Table 2. Table 3 lists the observed and calculated structure factors. Table 4 gives

Table 2. *Final atomic coordinates and thermal parameters* ($\times 10^4$)

Estimated standard deviations are in parentheses.

	x	y	z	β_{11}	β_{22}	β_{33}	β_{12}	β_{13}	β_{23}
Cl	0·7799 (3)	0·4799 (2)	0·4625 (1)	293 (5)	191 (4)	30 (0)	20 (3)	−22 (1)	−1 (1)
F	−1·3913 (5)	0·5558 (5)	−0·0277 (1)	262 (9)	378 (11)	22 (1)	−28 (8)	−2 (2)	28 (2)
O(1)	0·0229 (4)	0·7050 (4)	0·3079 (1)	196 (8)	36 (5)	22 (1)	24 (5)	21 (2)	−4 (2)
O(2)	−0·7452 (5)	0·6054 (5)	0·1607 (1)	217 (10)	132 (7)	21 (1)	14 (7)	18 (2)	−8 (2)
N	−0·2119 (6)	0·4373 (4)	0·2233 (2)	155 (10)	60 (6)	17 (1)	−12 (6)	17 (2)	5 (2)
C(1)	0·5761 (8)	0·4926 (7)	0·4181 (2)	216 (16)	100 (11)	20 (1)	9 (11)	4 (4)	3 (3)
C(2)	0·5417 (8)	0·4090 (7)	0·3766 (2)	212 (17)	84 (12)	22 (1)	41 (12)	17 (4)	2 (3)
C(3)	0·3845 (7)	0·4272 (6)	0·3401 (2)	181 (15)	77 (9)	18 (1)	10 (9)	8 (4)	−11 (3)
C(4)	0·2562 (7)	0·5291 (6)	0·3445 (2)	174 (14)	72 (10)	14 (1)	7 (9)	20 (3)	−3 (3)
C(5)	0·2932 (8)	0·6097 (7)	0·3878 (2)	239 (17)	149 (12)	17 (1)	41 (12)	18 (4)	−11 (3)
C(6)	0·4510 (9)	0·5933 (8)	0·4245 (2)	287 (18)	163 (13)	17 (1)	16 (13)	0 (4)	−16 (3)
C(7)	0·0938 (7)	0·5533 (6)	0·3042 (2)	146 (12)	46 (8)	18 (1)	3 (8)	19 (3)	1 (2)
C(8)	−0·0635 (7)	0·4518 (6)	0·3128 (2)	173 (12)	62 (8)	16 (1)	4 (8)	22 (3)	2 (2)
C(9)	−0·2363 (7)	0·4622 (6)	0·2721 (2)	177 (13)	61 (8)	17 (1)	−7 (9)	23 (3)	6 (2)
C(10)	−0·0804 (7)	0·5427 (5)	0·2144 (2)	151 (12)	50 (8)	17 (1)	−18 (8)	21 (3)	4 (2)
C(11)	0·0985 (7)	0·5282 (6)	0·2528 (2)	145 (12)	66 (8)	16 (1)	−6 (8)	22 (3)	−3 (2)
C(12)	−0·3791 (7)	0·4548 (6)	0·1838 (2)	157 (12)	70 (8)	17 (1)	−2 (8)	10 (3)	9 (2)
C(13)	−0·5299 (7)	0·3541 (6)	0·1894 (2)	154 (12)	74 (8)	21 (1)	1 (9)	20 (3)	13 (3)
C(14)	−0·6897 (7)	0·3536 (6)	0·1436 (2)	162 (13)	71 (9)	21 (1)	−10 (9)	17 (3)	4 (3)
C(15)	−0·7941 (8)	0·4972 (7)	0·1337 (2)	172 (14)	107 (10)	15 (1)	−4 (10)	26 (3)	1 (3)
C(16)	−0·9541 (7)	0·5065 (7)	0·0914 (2)	186 (13)	99 (10)	13 (1)	−15 (10)	17 (3)	6 (3)
C(17)	−1·0181 (8)	0·3894 (7)	0·0603 (2)	194 (14)	116 (11)	18 (1)	−19 (10)	14 (3)	7 (3)
C(18)	−1·1671 (9)	0·4041 (8)	0·0205 (2)	237 (16)	158 (13)	18 (1)	−73 (12)	14 (4)	−4 (3)
C(19)	−1·2505 (9)	0·5404 (10)	0·0128 (2)	196 (15)	242 (16)	15 (1)	−32 (13)	5 (3)	19 (4)
C(20)	−1·1928 (10)	0·6572 (9)	0·0430 (3)	247 (18)	205 (15)	22 (1)	75 (14)	12 (4)	16 (4)
C(21)	−1·0451 (9)	0·6407 (7)	0·0818 (2)	232 (16)	144 (11)	17 (1)	30 (11)	10 (4)	5 (3)

bond angles while Table 5 displays a comparison of the important torsional angles in I*a* and I*b*. Fig. 2 shows a stereoscopic view of a portion of the crystal structure of haloperidol.

As expected, the structures I*a* and I*b* are very similar. The molecular conformations, as revealed by the selected torsional angles in Table 5, are identical within experimental error.

Table 3. *Observed* ($\times 10$) *and calculated* ($\times 10$) *structure factors for haloperidol*

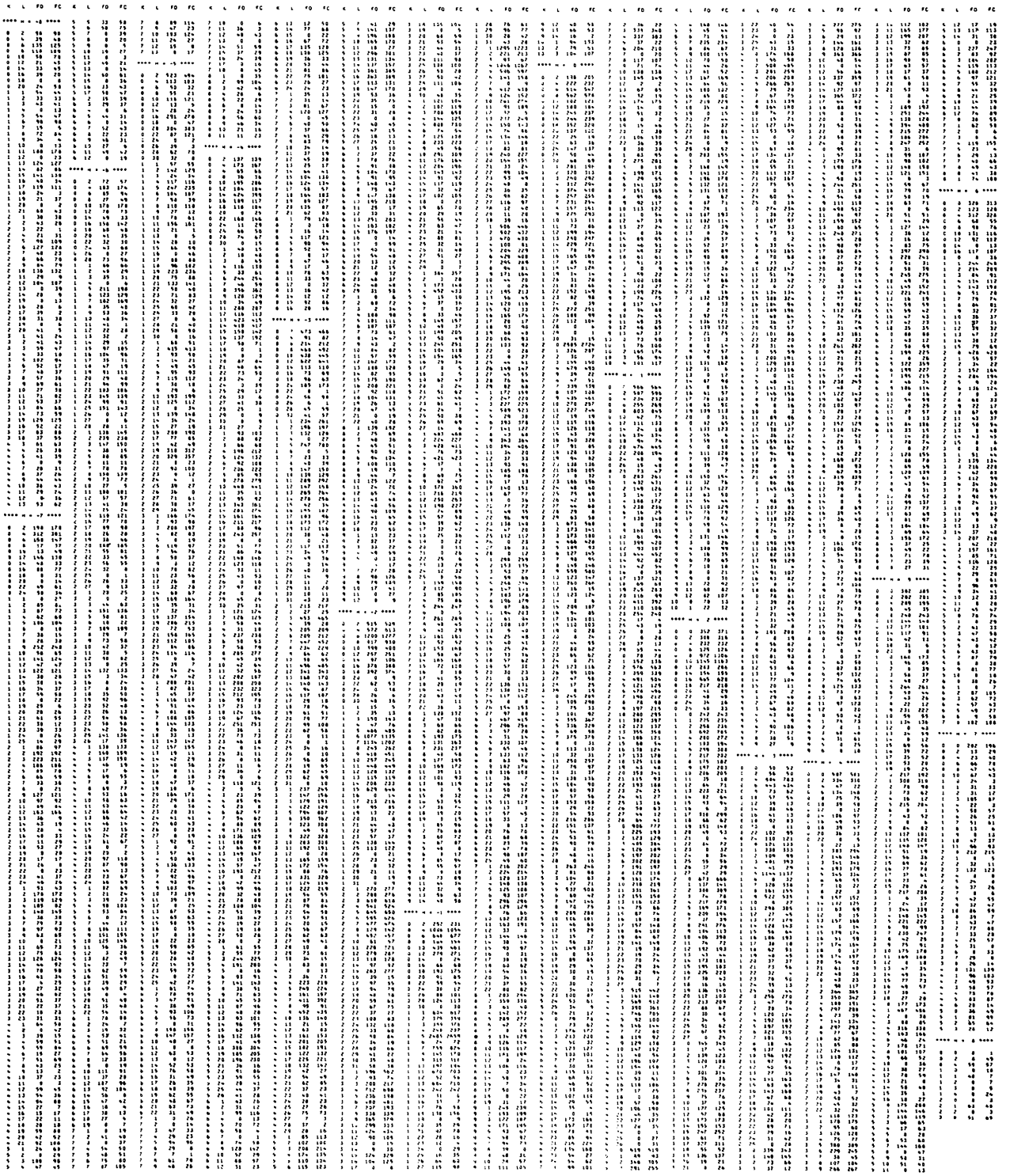

Table 4. *Bond angles for haloperidol*

Estimated standard deviations are in parentheses

Cl——C(1)—C(2)	120·7 (5)°	C(13)–C(12)–N	113·8 (5)°
Cl——C(1)—C(6)	119·1 (5)	C(12)–C(13)–C(14)	112·5 (5)
C(2)—C(1)—C(6)	120·1 (6)	C(13)–C(14)–C(15)	115·2 (5)
C(1)—C(2)—C(3)	120·2 (6)	C(14)–C(15)–C(16)	119·4 (6)
C(2)—C(3)—C(4)	121·7 (6)	C(14)–C(15)–O(2)	120·2 (6)
C(3)—C(4)—C(5)	116·6 (5)	C(15)–C(16)–C(17)	123·5 (6)
C(3)—C(4)—C(7)	122·5 (5)	C(15)–C(16)–C(21)	118·7 (6)
C(5)—C(4)—C(7)	120·8 (5)	C(17)–C(16)–C(21)	117·9 (6)
C(4)—C(5)—C(6)	122·1 (6)	C(16)–C(17)–C(18)	121·4 (6)
C(1)—C(6)—C(5)	119·1 (6)	C(16)–C(17)–O(2)	120·4 (6)
C(4)—C(7)—O(1)	108·6 (4)	C(17)–C(18)–C(19)	118·0 (6)
C(4)—C(7)—C(8)	110·0 (5)	C(18)–C(19)–C(20)	122·2 (6)
C(4)—C(7)—C(11)	114·4 (5)	F——C(19)–C(18)	117·5 (7)
C(8)—C(7)—O(1)	105·6 (4)	F——C(19)–C(20)	120·3 (8)
C(8)—C(7)—C(11)	109·0 (4)	C(19)–C(20)–C(21)	118·9 (7)
C(11)–C(7)—O(1)	108·8 (4)	C(16)–C(21)–C(20)	121·6 (7)
C(7)—C(8)—C(9)	113·0 (4)	C(9)—N——C(10)	110·3 (4)
C(8)—C(9)—N	112·6 (4)	C(9)—N——C(12)	112·2 (4)
C(11)–C(10)–N	111·6 (4)	C(10)–N——C(12)	108·3 (4)
C(7)—C(11)–C(10)	112·0 (5)		

Table 5. *Comparison of selected torsion angles*

Torsion angle is in degrees. In the sequence of atoms A–B–C–D, the clockwise rotation of C–D with respect to A–B when viewed along the B–C bond defines the positive torsion angle τ(ABCD).

	$C_{21}H_{23}O_2NF_2$*	$C_{21}H_{23}O_2NClF$
C(12)–C(13)–C(14)–C(15)	−68·2	−71·2
C(13)–C(14)–C(15)–C(16)	−177·5	−176·7
N——C(12)–C(13)–C(14)	−166·2	−168·7
C(5)—C(4)—C(7)—C(8)	−89·4	−87·7
C(5)—C(4)—C(7)—C(11)	151·8	148·9
C(3)—C(4)—C(7)—C(11)	−28·4	−31·4
C(3)—C(4)—C(7)—C(8)	90·9	92·0
C(5)—C(4)—C(7)—O(1)	27·9	27·9
C(3)—C(4)—C(7)—O(1)	−151·8	−152·4

* Recalculated from the data supplied by Koch (Koch & Germain, 1972).

These compounds, however, have measurable differences in pharmacological potency (increasing in the order $Y = H < F < Cl < CH_3$). Thus it would appear possible that any enhancement of activity in this series may be related to the steric and/or electronic nature of the Y group since it is demonstrated that the overall conformation of I*a* and I*b* in the solid state (as the free base) are the same.

The observed hydrogen bonding [O(1)···N, 2·84 Å] is identical to that determined for I*a*.

The two benzene rings are planar within experimental error and the observed distances and angles for the molecule are in good agreement with generally accepted values. No unusual intermolecular contacts were observed. The conformation of the piperidine ring is the expected chair form with the chlorophenyl group in the equatorial position and the hydroxyl group axially oriented.

The intermolecular hydrogen bonding between O(1) and N is shown in Fig. 2 (reference Fig. 1 for the numbering scheme). As expected, this hydrogen bonding pattern involves the piperidene ring nitrogen from the exposed face (*i.e.* in the orientation involving minimum axial hydrogen interactions).

A relationship between molecular conformation and biological activity of various pharmacologically active amines has been demonstrated (Camerman & Camerman, 1972; Chothia & Pauling, 1969). The emphasis of these studies has been directed toward determining what spatial similarities exist among various drug molecules that are generally quite unsimilar chemically but elicit a similar biological response such as (1) anticonvulsant activity, (2) acetylcholinesterase inhibition, and (3) psychotropic activity. While it appears that specific spatial arrangement of a small number of important atoms is responsible for specific activity in the first two classes above, such a relation has not been experimentally demonstrated for the third class. What has been shown for the haloperidol-like psychotropic

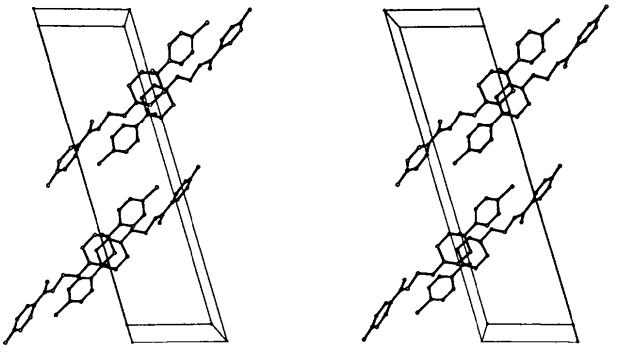

Fig. 2. A stereoscopic view of the crystal structure of haloperidol. For clarity, only a portion of the unit-cell contents is depicted, revealing the hydrogen bonding scheme.

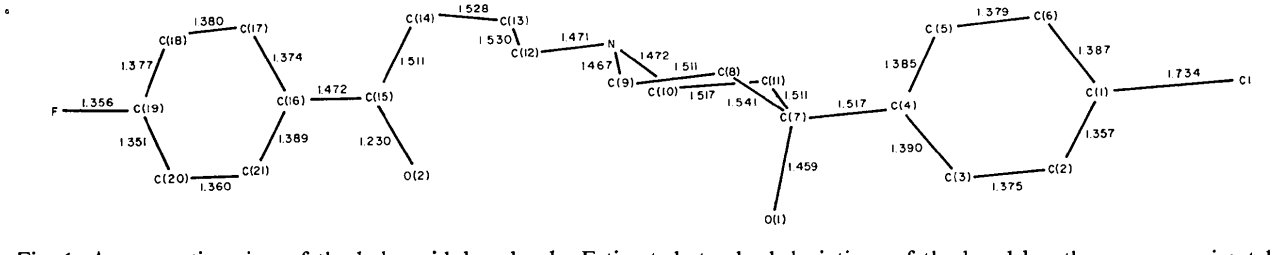

Fig. 1. A perspective view of the haloperidol molecule. Estimated standard deviations of the bond lengths are approximately 0·01 Å.

drugs is that the crystal forms for the free base and hydrochloride exist in distinctly different conformations (Koch & Germain, 1972). Considerations of this factor will be important in arriving at sound conclusions concerning the probable *in vivo* conformation of these molecules.

While the exact mode of action of these compounds is unknown, the study of molecules of equal or greater activity but possessing pronounced structural differences will help in establishing the essential conformational features required to produce biological activity.

We thank Drs C. Cain and J. Kleis of the McNeil Laboratories for supplying the material used in this investigation and the University of Arizona Computing Center for generous support.

Computer programs used in the solution, refinement, and analysis of this structure include: Raymond's *UCFACS*, Dewar's *FAME*, Germain's *MULTAN*, Zalkin's *FORDAP*, Busing & Levy's *ORFLS* and *ORFFE*, and Johnson's *ORTEP*.

References

CAMERMAN, N. & CAMERMAN, A. (1972). *J. Amer. Chem. Soc.* **94**, 8553–8556.
CHOTHIA, C. H. & PAULING, P. J. (1969). *Nature, Lond.* **223**, 919–921.
GERMAIN, G., MAIN, P. & WOOLFSON, M. M. (1970). *Acta Cryst.* B**26**, 274–285.
HANSON, H. P., HERMAN, F., LEA, J. D. & SKILLMAN, S. (1964). *Acta Cryst.* **17**, 1040–1044.
KARLE, J. & HAUPTMAN, H. (1956). *Acta Cryst.* **9**, 635–651.
KOCH, M. H. J. & GERMAIN, G. (1972). *Acta Cryst.* B**28**, 121–125.
SCHAEFER, J. P. (1967). *Chem. Commun.* pp. 743–744.

Acta Cryst. (1973). B**29**, 1890

Nouvel Affinement de la Structure Cristalline du Bis(pyridine-2 Carboxylato) Cuivre (II), Hydraté

PAR RENÉ FAURE, HENRI LOISELEUR ET GERMAINE THOMAS-DAVID

Laboratoire de Chimie Analytique II, *Université Claude Bernard, Lyon* I, 43 *boulevard du* 11 *Novembre* 1918, 69621 *Villeurbanne, France*

(*Reçu le* 1 *mars* 1973, *accepté le* 3 *mai* 1973)

Crystals of hydrated bis(pyridine-2-carboxylato)copper(II), also known as copper picolinate are triclinic, space group $P\bar{1}$: $a=5{\cdot}122$, $b=7{\cdot}717$, $c=9{\cdot}216$ Å; $\alpha=101{\cdot}07$, $\beta=95{\cdot}60$, $\gamma=101{\cdot}45°$ The structure was determined by means of a Patterson function calculated with intensities collected on an automatic four-circle diffractometer using Mo $K\bar{\alpha}$ radiation. The final R is 0·032 for the 2827 observed reflexions. The molecule is symmetrical around the copper atom, which is octahedrally coordinated by two nitrogen atoms, two carboxylic oxygen atoms and two other carboxylic oxygen atoms belonging to two molecules situated at $\pm a$ along [100]. The water molecules are in interstitial positions, making hydrogen bonds of two types: aqueous oxygen···carboxylic oxygen and aqueous oxygen···aqueous oxygen (with an equal distribution). These results and those of Takenaka, Utsumi, Yamamoto, Furusaki & Nitta [*Nippon Kagaku Zasshi* (1970), **91**(10), 928–935] are compared.

Introduction

La structure du picolate de cuivre a déjà été déterminée par Takenaka, Utsumi, Yamamoto, Furusaki & Nitta (1970) à partir d'intensités photographiques (λ Cu $K\bar{\alpha}$) estimées visuellement. Nous avions, dans le même temps, entrepris la résolution des structures du pyridyl-2 acétate de cuivre dihydraté (Faure & Loiseleur, 1972) et du picolate de cuivre. Une particularité intéressante pour ce picolate pouvait être d'élucider le taux d'hydratation trouvé variable selon les auteurs, les exemples les plus récents étant les suivants: anhydre (Kleinstein & Webb, 1971), monohydrate (D'Ascenzo & Wendlandt, 1970), dihydrate (Gillard, Laurie & Stephens, 1968). Pour notre part, selon le mode de préparation décrit précédemment (Thomas, 1960), nous avons obtenu, par analyse thermogravimétrique, un taux d'hydratation pouvant varier selon les conditions atmosphériques (humidité, température) entre zéro et deux molécules d'eau (Faure, 1973). Nos résultats seront comparés à ceux obtenus par Takenaka *et al.* (1970).

Données expérimentales

Groupe $P\bar{1}$

$a=$ 5,122	$b=$ 7,717	$c=$ 9,216 Å
$\alpha=101{,}07$	$\beta=95{,}60$	$\gamma=110{,}45°$
$V=329{,}6$ Å^3	$M=343{,}54$	
$D_m=1{,}72$	$D_c=1{,}73$ g cm^{-3}	$Z=1$
$F(000)=175$	$\mu=17{,}5$ cm^{-1}	(λ Mo $K\bar{\alpha}$)